Environmental Energy and Economic Research 2022 6(3): S040
DOI 10.22097/eeer.2022.316215.1232

Research Article

Cost-Effective Dual-Axis Solar Tracker with Enhanced Performance

Amirhossein Fathi [a], Hossein Yousefi [b,*], Amirmahdi Komarizadeh [c], Mohammad Salehi [d], Kianoosh Choubineh [b], Laleh Ghahremani[e]

[a] School of Mechanical Engineering, Shiraz University, Shiraz, Iran.
[b] Department of Renewable Energies and Environment, Faculty of New Sciences and Technologies, University of Tehran, Tehran, Iran.
[c] Faculty of Natural Resources and Environment, Islamic Azad University Science and Research Branch, Tehran, Iran.
[d] Department of Energy Engineering, Sharif University of Technology, Tehran, Iran.
[e] Department of Mining Engineering, Isafahan University of Technology, Isafahan, Iran.

Received: 15 December 2021 /Accepted: 4 May 2022

Abstract

This paper presents a solar tracker which operates in altazimuth and polar mounts. Online calculation of the system's optimal position better utilizes the tracker in different regions and climates. The system is designed to be easily assembled or disassembled, and each piece of equipment is accessible. The tacker has the best performance in various environments and locations, and the optimal position is determined online by a pair of light-dependent resistors (LDRs) on its appropriate structure. Restricting the path in which the system traces the sun by installing two micro keys reduces actuators' power considerably. The rotation period is not the same for each climate and location to improve the net efficiency. To improve the net efficiency, the rotation period is not the same for each climate and location. There are three methods to calibrate the structure and sensors: balance weight, LDRs' base, and adjusting LDRs' resistance. This tracker's performance was tested against a fixed system in various weather conditions. On a cloudy and rainy day, the two systems' output energy was equal. The net generated electricity increased to 24.6% on a sunny autumn day by defining the right hysteresis, while the global tilted irradiation increased by 34.7%. However, in the solar tracker's continuous working case, the net generated electricity could be 18.0% lower than utilizing the fixed structure.

Keywords: Calibration, dual-axis solar tracker, efficiency improvement, photovoltaic panel, solar irradiation

Introduction

Greenhouse gas (GHG) emissions are the root cause of climate change. This phenomenon has damaging effects on the planet and societies and is among the top human concerns (Change et al., 2006; Yousefi et al., 2019). To alleviate these problems, emissions have to be considerably cut to reach Paris Agreement's goals, curbing global temperature increase to well below 2 degrees Celsius (Rogelj et al., 2016). Climate change and other global energy crises have forced

* Corresponding Author E-mail: hosseinyousefi@ut.ac.ir

countries to implement policies like replacing renewable resources, reducing energy consumption, saving energy strategies, or controlling supply and demand (Esmailnejad, 2021). One of the great ways to achieve the agreement's aims is by using renewable energies to provide energy demand (Salehi et al., 2019). Because of their characteristics, such as being clean, unlimited, and uniformly distributed (Abdelghani-Idrissi et al., 2018), they do not give off operational greenhouse gases (Twidell and Weir, 2015). Their growth is projected to be noticeable during the next decades, becoming the dominant primary energy provider. Also, public acceptance and willingness to use these resources have risen (Komendantova and Yazdanpanah, 2017). Renewable energy proportion, consisting of wind, solar, geothermal, and bioenergy, will increase from five per cent in 2018 to around 40 or 60 % in 2040, depending on different scenarios (Outlook, 2020). The renewable energy capacity rose to around 260 GW in 2020, breaking the previous record in 2019 by almost 50 per cent (IRENA, 2021). The electricity generation from renewable sources climbed to 29 % in 2020, two per cent more than the year before (IEA, 2021). Solar energy plays a vital role in decreasing GHG, while solar's fraction of supplying energy is estimated to rise during the next thirty years due to plunging its cost by roughly a third (Creutzig et al., 2017; Outlook, 2020).

This energy has some merits, such as a low maintenance cost, installation in remote locations, and no operational environmental externalities (Hoffmann et al., 2018; Serrano-Luján et al., 2017). Solar Photovoltaic (PV) and solar thermal are two ways of harnessing the sun's energy (Letcher, 2018). The former is used to produce electricity. Solar PV is Iran's best sustainable development option (Rezaei, 2021). They emit lower GHGs during their life cycle than gas power plants (Nabi Bidhendi et al., 2021). Low energy density and the time difference between electricity production and consumption are the key challenges (Letcher, 2018). Moreover, PV systems suffer from low efficiency mostly because of fixed structures (Carvalho et al., 2013). There are four general strategies to improve PV power plants' efficiency: using technologies with higher energy efficiency, implementing solar tracking systems, adjusting the ratio between panels' capacity and inverter, and cooling panels' surface (Clifford and Eastwood, 2004; Elibol et al., 2017; Kerekes et al., 2009; Stritih, 2016). Other methods like floating panels could improve efficiency (Sadeghi and Vahidi, 2020). Fixed structures have been used for PV panels to produce electricity. However, tracking systems, which follow the sun's position, are gaining attention for their improved efficiency. This strategy generally boosts efficiency up to 40 % or even more in some cases (Abdelghani-Idrissi et al., 2018; Eldin, et al., 2016).

They use a single- or dual-axis scheme (Awasthi et al., 2020). The single-axis plan rotates to align the panel perpendicularly to the sun's radiation, in which the north meridian axis is suggested as the better option (Mousazadeh et al., 2009). The complex dual-axis scheme would have the highest efficiency because of more mechanisms, higher expenses, or dependability on geographical features (Awasthi et al., 2020). The solar trackers can be classified as their driving system: passive and active (Awasthi et al., 2020). While the first strategy does not have mechanical drivers, the second utilizes electrical drives and mechanical gear trains to follow the sun.

Several studies present different designs, testing, and modelling for enhancing the efficiency of PV panels. A passive solar tracker, not consuming energy from the panel itself, increased the efficiency by up to 23 % (Clifford and Eastwood, 2004). Not having a night return mechanism and a fixed tilted axis were the problems of this design. While a virtual polar dual-axis simulation brought opportunities for the optimal controller, changing elements, or the PV system (Alexandru and Pozna, 2010), the suggested system's test field could have introduced a better perspective and practicality.

The external disturbances, such as mechanical friction, wind loading, and the result averaging performed each hour, can cause discrepancies between an active single-axis tracker

and its computer simulation (Chin et al., 2011). An approach controlling the solar panel's movement was presented that grew a dual-axis solar tracker's response, rotating in azimuth and elevation direction (Ozcelik et al., 2011). U-PRU-PUS parallel mechanism to deal with the environment, load capacity, and stability raised the tracking range by nearly five per cent (Du et al., 2021). Cost is also significant in the tracker's structure. A low-profile two-axis solar tracker, including two coplanar and perpendicular linear actuators coupled with a linkage arm and pivot points atop actuator shuttles, can reduce the expenses (Barker et al., 2013). A mono-axial tracking system's analysis, using a single-open-loop model with a PID controller, showed an annual average efficiency of around 35% (Alexandru and Irina Tatu, 2013).

A simple active dual-axis solar tracker, having fewer components, was tested to produce approximately 36 % more energy, and it could be simply carried out (Hammoumi et al., 2018). Controlling the angle deviation within a polar single axis configuration optimized the harnessing of solar energy with fewer panel displacements (de Sá Campos and Tiba, 2021). Comparing a two-axis tracker with the fixed one implied an average monthly gain of between 18 to 32 % in Brazil (Hoffmann et al., 2018). This scheme had two perpendicular sets of engines, including the north-south and east-west directions. A discrete single-axis solar tracking system, actuating three times a day in the azimuthal plane, showed no differences in total solar energy generation when using tracking angles (Batayneh, et al., 2019). Following the sun at three optimized angles, this system collected 90 % more solar energy against a continuous single-axis solar tracker, moving three times an hour based on solar calculations. Using Light Dependent Resistor (LDR) sensors as the input, an automatic dual-axis solar tracker could increase the electrical efficiency by nearly 45 % (Jamroen et al., 2020). A bimetallic strip-driven solar tracking device with bistable laminates was produced to slash structure numbers (Zhang et al., 2020). It lowered the expenses and the tracker's general complexity, making it possible for use in engineering fields. Adaptive Neural Fuzzy Inference System was utilized to control solar tracking systems, which calculated the optimal tilt and orientation angles (AL-Rousan et al., 2020). Serial mechanisms in solar trackers limit load capacity and stability. A U-PRU-PUS parallel mechanism can deal with this setback (Du et al., 2021). The test revealed the tracking error was less than 2°. The Global Positioning System with Real-Time Clock could follow the sun in low light (Wu et al., 2022). The fiel measurement of this dual-axis tracker improved efficiency by around 36 %.

Studies showed that the cost is imperative (Fathabadi, 2016). Compared with fixed structures, either single- or dual-axis solar trackers require additional parts and apparatus. Even though this equipment raises the production cost, they enhance a PV system's efficiency. This increase in efficiency can translate into money, such as selling electricity to the network. Hence, a tracker is favourable when its investment, production, and operating expenses are low and its improved revenue is high. Still, any solar tracker should be compact because it occupies a larger space, if bulky, meaning higher cost buying or lending land.

The other important aspect of these systems is using an electric motor for following the sun's trajectory. As evident, the actuator consumes electricity in most cases from the PV panel, ranging between five to 10 per cent of the produced energy (Eldin et al., 2016). This energy consumption can even make tracking methods infeasible in some circumstances. The moving system's electricity should be the minimum amount to maximize the tracker's efficiency, meaning the motor's power is also the least. Investment and operational costs, therefore, are lower.

The study's novelties are a straightforward installation structure with available equipment and a simple control system with higher reliability, acceptable for remote areas. The tracker's frame, shown in the figures, mainly is from accessible water pipes and joints, and even an inexperienced person can assemble or dismantle the system. The resistance's capacity comes from a simulation model regarding the control system and hysteresis. Employing the advantages

of online and offline control systems is the main idea used in the control system. The vicinity of points is assessed by the offline method, and climate changes are then adjusted through the online one. Iran can be classified into five regions based on a simulation model developed for this country and its various climates. Adjusting the regions into five resistances equalizes the local optimal point to the global one. Hence, commercial manufacturing of this production is feasible.

The planning of a tracker could focus on its structure and control system. Generally, these systems' structure is more complex and expensive due to heavier load than the fixed systems. The control scheme can also have different levels based on various intricacies and costs. One of the primary purposes of this article is easy assembling and disassembling of the system with accessible equipment, leading to expenses and installing cost reduction because there is no requiring specialized workers. Mathematical programming initially determines the control strategy, and then other methods like trial and error adjust the optimal point. Although this approach results in lower different costs with higher reliability, the efficiency is relatively noticeable. Limiting the rotation path reduces the actuator's energy use, meaning lower investment cost, and improves the net efficiency of power plants.

This paper introduces a dual-axis solar tracker whose driving system is active. This system can operate in two different ways, which allows comparing these coordinate systems. Then, its components, control algorithm, and production are explained. Finally, its equipment and cost estimation and the empirical data of this system in comparison to a fixed system are presented.

Modeling

Although the sun's path is on a non-flat curve, the equatorial coordinate system with a single motor can trace the sun. This system is designed to operate on both altazimuth and polar mounts to compare their effects. A transporter inclines the central axis in altazimuth mount towards the Pole star. Figure 1 delineates its plan for holding two PV panels.

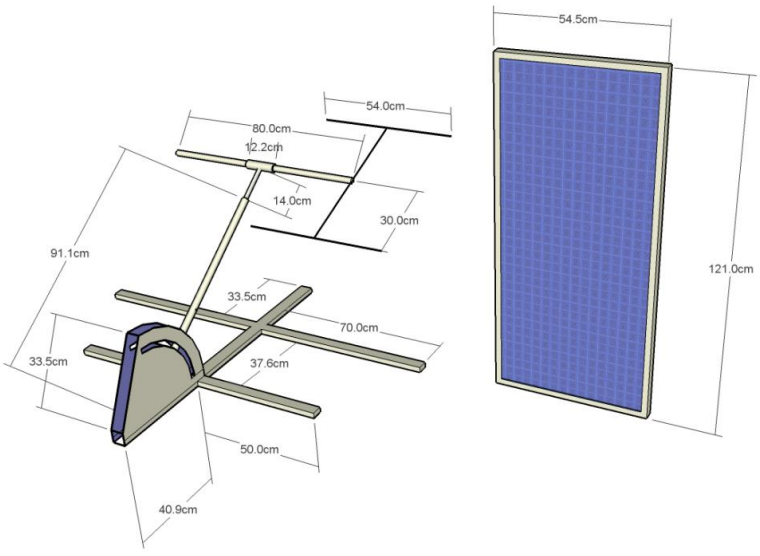

Figure 1. The system's stand with altazimuth and polar mounts for holding two PV panels

In this study, the tracker's performance is optimized with a hysteresis arrangement based on trial and error.

Although constant following the sun increases the input energy on panels, this preservation raises actuators' energy use and creates more vibrations. To prevent these circumstances, the system pursues the sun during specific periods

Tracker's Components

The main section, moving part, electronic equipment, and mechanical structure form the tracker.

Moving Part

This part involves two DC gear head actuators with six rpm speed. The sprocket is responsible for transferring power from motors into the system's axes. The gears ratio is 15 to 35.

Selected drivers for motors are two L293D Integrated Circuits (IC). These ICs provide the maximum current of 600 milliamperes (mA) permanently and 1 Ampere (A) instantly to control the actuator. Each actuator's power is about 12 W. These drivers are connected through H-Bridge, whose advantage is its easy joining compared to other models.

Measuring Devices

In this study, there are five types of sensors, including solar positioner, temperature, voltage, current, and spotting the path's end.

- *Solar Positioner Sensor*

Four photoresistors are used to position the sun: two for azimuth movement and the other two for elevation movement in altazimuth mount. These sensors are on lead screw nuts, and the pair of them are separated by a retaining plate, depicted in figure 2.

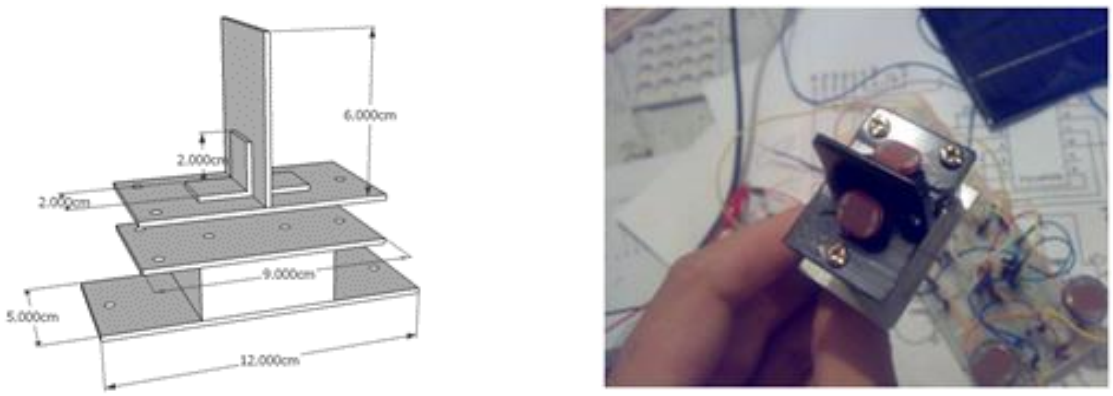

Figure 2. The stand of photoresistors solar positioning with three lead screw nuts for mechanical calibration

- *Voltage Sensor*

Considering common limitations of the voltage evaluation in commercial online monitoring systems, dividing the resistances is suggested for increasing the range of determining potential differences.

The main voltage is calculated as equation 1.

$$V_{out} = \frac{R_1}{R_1 + R_2} V_i \quad (2)$$

Where, V_i is the section's voltage, such as PV panel, and V_{out} is the measured voltage by monitoring. These two variables can be transformed into each other by equation 2.

- *Current Sensor*

There are two methods for deciding the current: conversing current to voltage using resistance or Hall effect sensor. This paper calculates the current through the former approach with the ACS712 sensor.

- *Spotting the Path's End*

The path's end is an encounter point where a micro key is on the structure's eastern and western sides. The encounter cuts off the input power of the actuator. This idea limits the start and endpoint of the distance panel should go through, reducing the power and, hence, the electricity of the actuator. The keys shorten the interval between each tracker due to diminished shadow length. Also, strong winds or an obstacle blocking the tracker's path cannot put excessive pressure on the system and disrupt its functioning.

Control Algorithm

Two pairs of Light-Dependent Resistors (LDR) detect the sun's trajectory, placing 90 degrees respecting each other, illustrated in figure 2. Its electrical resistivity logarithmically decreases with growing radiant intensity.

The control circuit compares the two sensor's resistance, and any side with a lower resistivity translates into that the sun is there. Commands are then sent to move panels in that direction. Motion in the other direction, azimuth-elevation mount, is likewise established by sensors and corresponding motor. The control circuit's schematic plan is specified in figure 3.

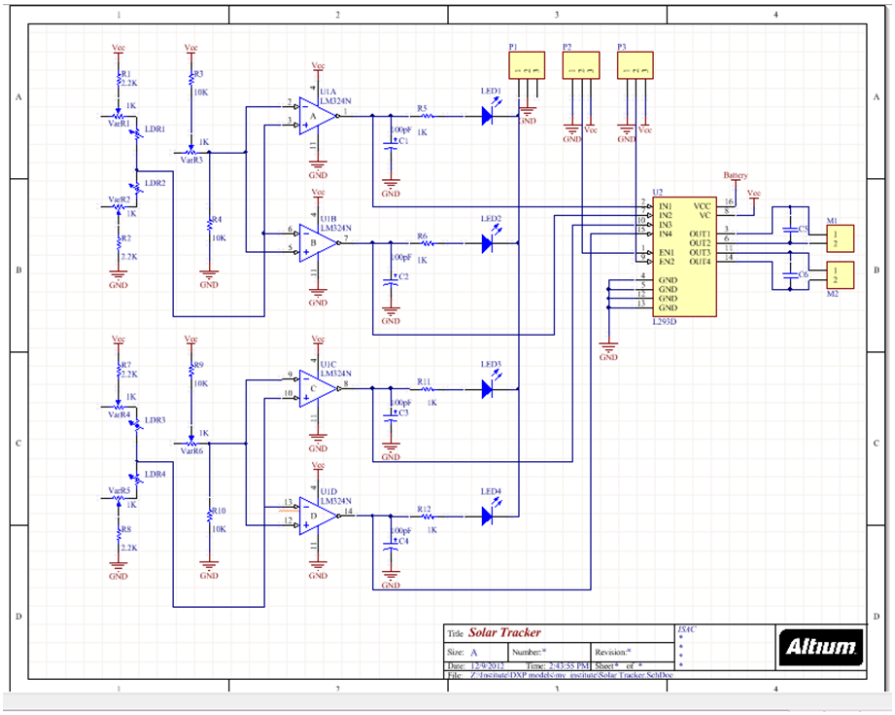

Figure 3. Schematic circuit of the solar tracker

R_1 and R_2 resistances, each 2.2 $k\Omega$, restrict the current over solar positioner sensors. Their value will be equal if the received radiant intensity to everyone is the same, denoting the point A's voltage is half of V_{cc}. Changing the $VarR_1$ or $VarR_2$ potentiometer breaks the equality. Therefore, these potentiometers manage the optical sensors' calibration. Point A is connected to the first and second comparators' positive and negative rails, respectively, using IC with the LM324 number and four comparators. Because of the $VarR_3$ potentiometer between the first and second comparators' negative and positive rails, there is a voltage difference between these two rails. If it is zero, the first comparator's voltage is equal but opposite to the second's one, and its quantity is $\frac{V_{cc}}{2}$, the same as point A. A slight change in the photoresistor's amount starts the actuator that culminates in panels sticking to the sun's path. But as long as radiation variation is little, PV panels can not go further from their initiate point, and thus, the motor direction becomes reverse. This fluctuates around the maximum point of light forever. The

fluctuation is clearly visible because the mechanical system has relatively high inertia. Now, if the amount of $VarR_3$ is zero, there would be a voltage difference between the first comparator's negative rail and the second's positive one, named Hysteresis Voltage. The radiation variation has to be that point A's voltage exceeds $\frac{V_{cc}}{2} + V_{hysteresis}$ which generates no fluctuations. The greater the *Var*'s amount, the higher $V_{hysteresis}$ and the lower the system's sensitivity to light change. The comparators' outputs are sent to two buffers with an IC number of L293D, and the buffer's output is connected to the motor via H-Bridge. There is the same circuit for the altazimuth mount.

Solar Tracker Production

The solar tracker production consists of two stages: mechanical and control.

Mechanical Stage

The main base and axis, the primary and secondary axis motor system, and balance components are three pieces of this stage.

- *The Main Base and Axis*

It is for both mounts and has a main axis, coupling, ball bearing, position adjustment screw, conveyer plate, fixed base, wheel for transportation, H-base, and apparatus for holding the controller.

- *The axis motor system*

It contains the primary and secondary systems. The primary is for choosing azimuth movement or solid angle. LDR sensor and its adjusting piece, sprocket, DC motor, and gearbox form the primary system, showed in figure 4.

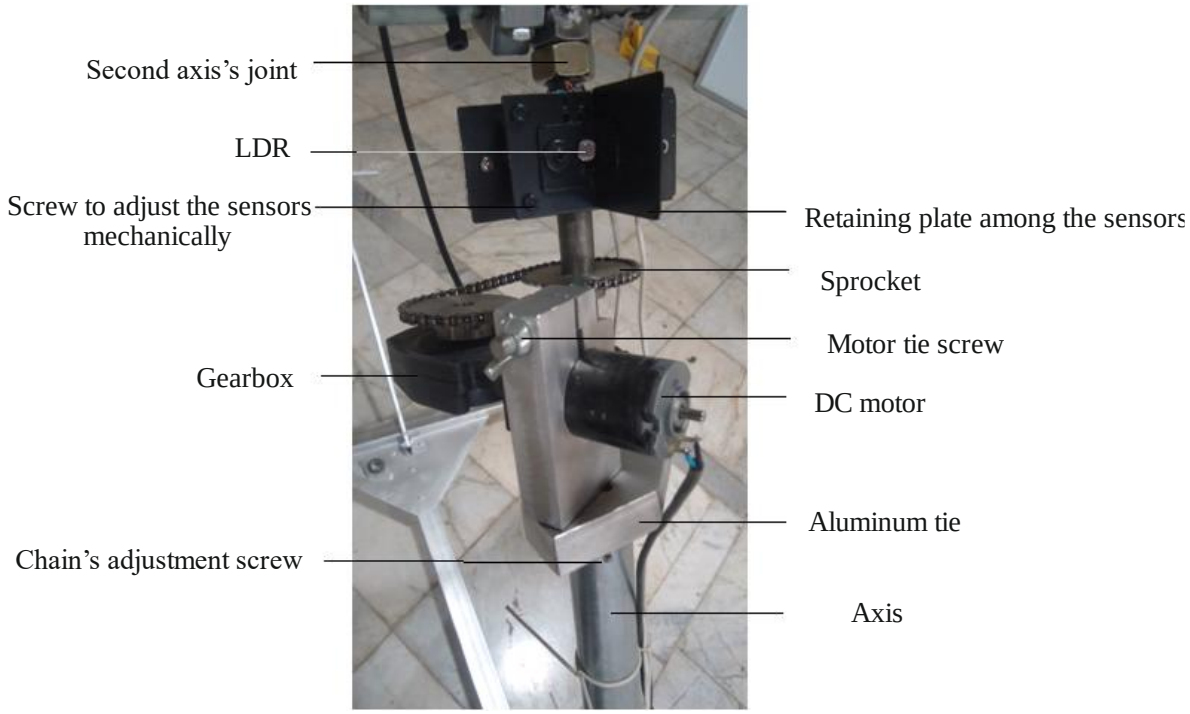

Figure 4. Moving parts of the primary axis of the solar tracker

The second system pursues the sun's elevation in the altazimuth mount and its declination in the equatorial mount. This piece involves the LDR sensor and its parts for adjusting the DC motor, sprocket, and gearbox. Figure 5 indicates this system.

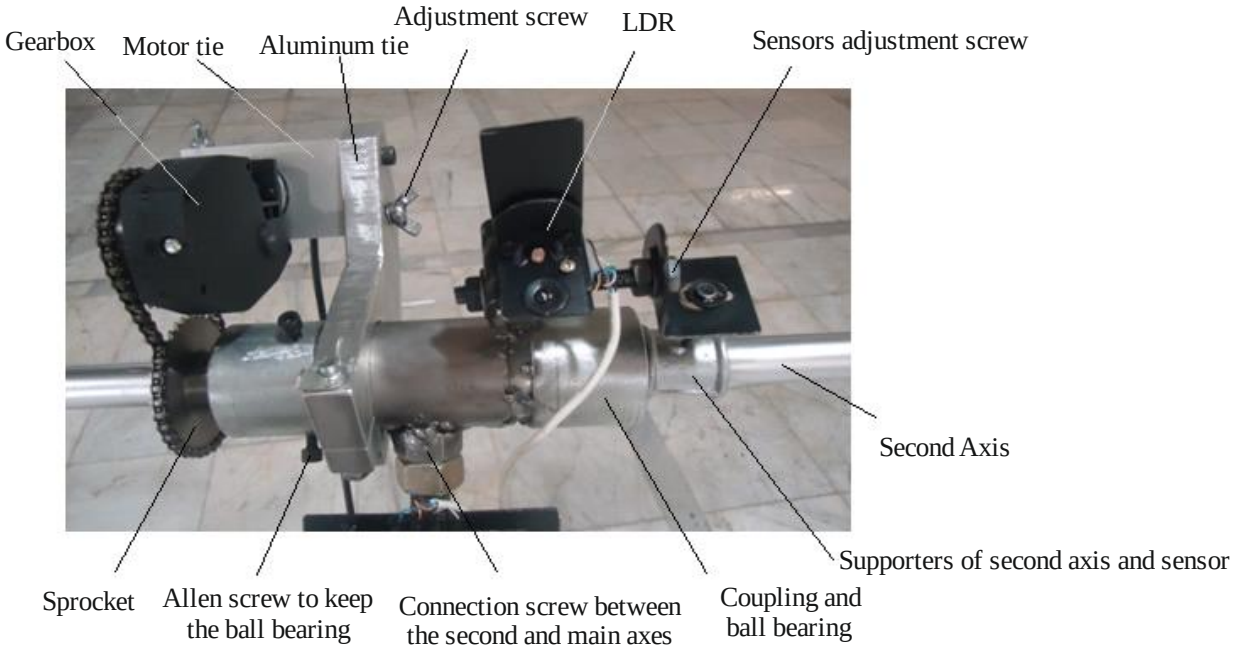

Figure 5. Moving parts of the secondary axis of the solar tracker

- *Balance Components*

Including two 0.5 kg weights, this stage maintains the balance of the tracker. These two weights are joined with a rod.

Control Section

The controller has the following sun electronic circuits, a day and night sensor, and displays for currents and voltages of actuators and PVs. Two controller boxes are arranged: one for the tracker circuit, monitoring information, the day and night sensor, displays of currents and voltages and connection plugs, and the other just for monitoring's data of panels. The control box is presented in Figure 6.

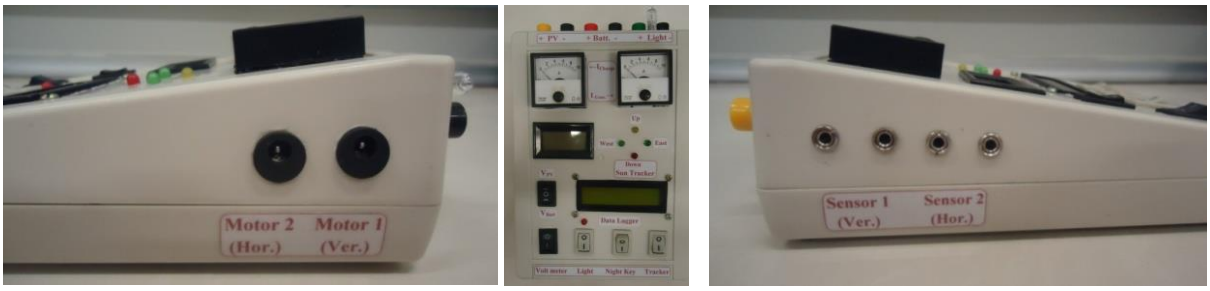

Figure 6. Control box of the tracker equipped with online monitoring

In the output division, Light, the box has a halogen lamp key to compare with an LED with the matching power.

A lighting key in the box automatically turns on the lighting system when the sky goes dark, illuminating the outdoor space. Its circuit has a comparator between the panel and battery voltage to determine day and night.

Results

The solar tracker's structure is designed based on two 80 Watts panels; their features are presented in table 1.

The equipment for manufacturing the tracker and the online monitoring system with related costs are introduced in table 2.

Table 1. The panel specifications

Company	**Sharp**
Model	NE-080T1J
Dimensions	1214*545*35mm
Weight	9 kg

Table 2. Component costs

	Equipment	**Description**	**Unit Price ($)**	**Number**	**Cost Estimation ($)**
1	Iron tools	Base and Stand	50	1	50
2	Motor Tie	Aluminum	10	2	20
3	Gear	3 cm Diameter	5	2	10
4	Gear	10 cm Diameter	15	2	30
5	Chain	Galvanized	3	2	6
6	Ball Bearing	20.50 mm	2	2	4
7	Ball Bearing	22.50 mm	2	2	4
8	PV Support	Pipes, Joints, Taps	50	2	100
9	DC Gearhead Motor	12rpm	20	2	40
10	Sun Tracker Board	Two Channels with Multi-Turn Calibration	25	1	25
11	Light Key Board	PV sensor	10	1	10
12	Pair of Optical Sensor	With Mechanical Calibration	0.5	2	1
13	Data Logger Board		45	2	90
14	Evaluation Board		40	2	80
15	Voltage Sensor		1	4	4
16	Current Sensor		2	4	8
17	Current Sensor's Circuit		2	1	2
18	Temperature Sensor		1	2	2
19	Control Box		10	1	10

The prices reported in Table 2 are from a retailer in Tehran, Iran. A survey on the market reveals that there is a noticeable difference between this table's providers with others.

The tracking system and a fixed one, with the same traits stated in Table 1, were erected side by side to examine their performance, depicted in Figure 7. The fixed structure was installed on the second terrace's edge of Sharif Research Institute, with 54 degrees between the panel's normal vector and the horizon. Tests were executed in three different set-ups: fixed, altazimuth, and polar mounts.

The panel's outputs went into a $2.2k\Omega$ resistance, 100 Watts, like 30 cm of a heating element. The reason behind using a resistance load instead of charging a battery was the discrepancy in

the initial batteries' initial charge. These differences might have created less battery charging into produced electricity by PVs.

The two mounts trace the sun, and altazimuth's motors consume at least twice the electricity compared to the other. While the altazimuth's path is winding, the equatorial mount's route just rotates two-degree every week.

The solar tracker's performance is assessed on sunny days. Figures 8 and 9 report the recorded voltage and current of the two systems' panels.

Figure 7. The test of comparing and collecting data of the tracker and fixed systems in the equatorial mount

The system's performance on a sunny day

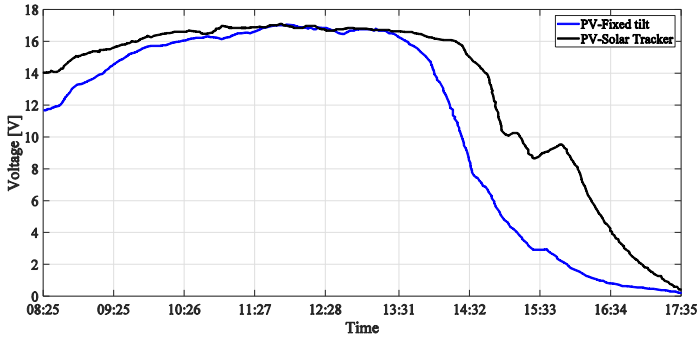

Figure 8. The recorded voltage of the fixed and tracking systems

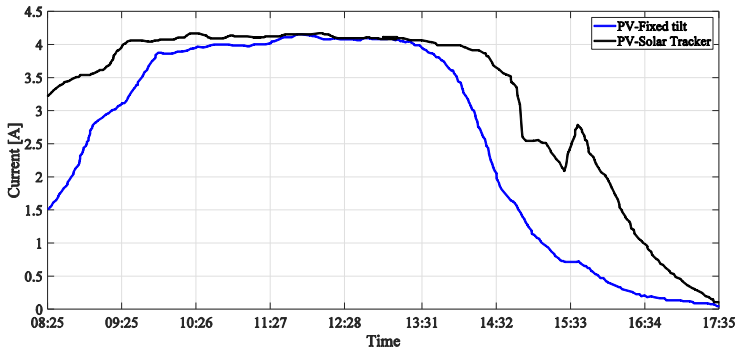

Figure 9. The recorded current of the fixed and tracking systems

Briefly, it could be concluded that the tracker raises the input energy by 34.7%. This growth provokes the generated electricity from the panels to improve by 22.3% and 24.6% in the first and second scenarios, respectively, when the actuators do not work continuously. Still, when the actuators work constantly, the generated electricity in the third scenario is reduced by -18.0% compared to the fixed structure. Furthermore, the increment in the fourth scenario is about 4.3%. If the tracker continuously follows the sun, there is a possibility that the increased

input energy is less than the energy consumed by the system during the lower radiation times of a day. The developed tracking system's efficiency is acceptable compared to the previous studies, although the test's conditions are different, such as climate, positioning, tracker, or panel. For example, the following studies (Alexandru and Irina Tatu, 2013; Clifford and Eastwood, 2004; Hammoumi et al., 2018; Hoffmann et al., 2018) demonstrated efficiency improvement by 23, 35, 18 to 32, and 36 %, respectively. It is worth mentioning that some did not report the gross production, meaning not subtracting the actuator's consumption from the panel's production.Most of the equipment installed on the structure and the tracking system is based on educational purposes. In reality, there is no need for monitoring, actuator, strong gearbox, or other tools. Besides, the two panels were produced in 2012. the tracker's cost, including adjusting the tracking structure, for the panel set of 250 W was around 100 $. 18 % increase in average annual production, 20 % average capacity factor, and 0.1 $/kWh resulted in a 12-year and 8-month return period. The tracker can cause improved annual production. If the panels are replaced with newer versions, each system will decrease greenhouse gas emissions by 100 kg annually, considering 1.3 $\frac{kg_{CO_2}}{kWh}$ (Kodra et al., 2015). It is evident that changing the system's location will influence annual production.

Conclusion

This paper introduces a novel dual-axis solar tracker with one stand, providing the ability to move in two different mounts. The tracking design can be easily implemented with available apparatus, and even an inexperienced person can assemble or dismantle the system. In order to enhance efficiency in the control system, two micro keys are added at the end of the rotation path for reducing energy use. Attaching the micro key to the moving part determines the path's finishing point, and the rotation's direction is reversed when the shadow is on panels. A pair of LDRs decides the optimal position. There are three methods for calibrating this tracking system: balance weights installed on the structure, LDRs' base, and adjusting LDRs' resistance with Multimeter. The solar tracker's electrical output power was compared with a fixed system whose angle can be changed in several situations. The two systems' output power was similar on a cloudy day, meaning that the system was calibrated correctly and the control strategy worked well. On a sunny autumn day, the global tilted irradiation on the panels increases by 34.7% compared to the panels installed on the fixed structure that leads the net produced electricity went up by 24.6 %. If the actuators work in the optimum step size, the production can be lower than the fixed structure. Not having access to suitable DC motors can affect the results, and if the proper ones had been used, there would have been a more significant increase in produced net electricity.

Reference

Abdelghani-Idrissi, M. A., Khalfallaoui, S., Seguin, D., Vernières-Hassimi, L., and Leveneur, S. (2018). Solar tracker for enhancement of the thermal efficiency of solar water heating system. Renewable Energy, 119, 79–94.

AL-Rousan, N. A., Isa, N. A. M., and Desa, M. K. M. (2020). Efficient Single and Dual Axis Solar Tracking System Controllers Based on Adaptive Neural Fuzzy Inference System. Journal of King Saud University-Engineering Sciences.

Alexandru, C, and Pozna, C. (2010). Simulation of a dual-axis solar tracker for improving the performance of a photovoltaic panel. Proceedings of the Institution of Mechanical Engineers, Part A: Journal of Power and Energy, 224(6), 797–811.

Alexandru, C., and Irina Tatu, N. (2013). Optimal design of the solar tracker used for a photovoltaic string. Journal of Renewable and Sustainable Energy, 5(2), 23133.

Awasthi, A., Shukla, A. K., SR, M. M., Dondariya, C., Shukla, K. N., Porwal, D., and Richhariya, G.

(2020). Review on sun tracking technology in solar PV system. Energy Reports, 6, 392–405.
Barker, L., Neber, M., and Lee, H. (2013). Design of a low-profile two-axis solar tracker. Solar Energy, 97, 569–576.
Batayneh, W., Bataineh, A., Soliman, I., and Hafees, S. A. (2019). Investigation of a single-axis discrete solar tracking system for reduced actuations and maximum energy collection. Automation in Construction, 98, 102–109.
Carvalho, D. R., Lacerda Filho, A. F., Resende, R. C., Possi, M. A., and Kruckeberg, J. P. (2013). An economical, two axes solar tracking system for implementation in Brazil. Applied Engineering in Agriculture, 29(1), 123–128.
Change, A. D. C., Blair, T., and Pachauri, R. (2006). Avoiding dangerous climate change. Cambridge University Press.
Chin, C. S., Babu, A., and McBride, W. (2011). Design, modeling and testing of a standalone single axis active solar tracker using MATLAB/Simulink. Renewable Energy, 36(11), 3075–3090.
Clifford, M. J., and Eastwood, D. (2004). Design of a novel passive solar tracker. Solar Energy, 77(3), 269–280.
Creutzig, F., Agoston, P., Goldschmidt, J. C., Luderer, G., Nemet, G., and Pietzcker, R. C. (2017). The underestimated potential of solar energy to mitigate climate change. Nature Energy, 2(9), 17140.
de Sá Campos, M. H., and Tiba, C. (2021). npTrack: A n-Position Single Axis Solar Tracker Model for Optimized Energy Collection. Energies, 14(4), 925.
Du, X., Li, Y., Wang, P., Ma, Z., Li, D., and Wu, C. (2021). Design and optimization of solar tracker with U-PRU-PUS parallel mechanism. Mechanism and Machine Theory, 155, 104107.
Eldin, S. A. S., Abd-Elhady, M. S., and Kandil, H. A. (2016). Feasibility of solar tracking systems for PV panels in hot and cold regions. Renewable Energy, 85, 228–233.
Elibol, E., Özmen, Ö. T., Tutkun, N., and Köysal, O. (2017). Outdoor performance analysis of different PV panel types. Renewable and Sustainable Energy Reviews, 67, 651–661.
Esmailnejad, M. (2021). Wind Energy Potential for Providing Small Wind Energy Systems to Generate Electricity in Residential and Agricultural Areas in Southeastern Iran. Environmental Energy and Economic Research, 5(3), 1–16.
Fathabadi, H. (2016). Novel high efficient offline sensorless dual-axis solar tracker for using in photovoltaic systems and solar concentrators. Renewable Energy, 95, 485–494.
Hammoumi, A. E., Motahhir, S., Ghzizal, A. El, Chalh, A., and Derouich, A. (2018). A simple and low- cost active dual- axis solar tracker. Energy Science and Engineering, 6(5), 607–620.
Hoffmann, F. M., Molz, R. F., Kothe, J. V., Nara, E. O. B., and Tedesco, L. P. C. (2018). Monthly profile analysis based on a two-axis solar tracker proposal for photovoltaic panels. Renewable Energy, 115, 750–759.
IEA. (2021). Global Energy Review 2021. Retrieved from https://www.iea.org/reports/global-energy-review-2021/renewables
IRENA. (2021). Renewable Capacity Statistics 2021. Abu Dhabi.
Jamroen, C., Komkum, P., Kohsri, S., Himananto, W., Panupintu, S., and Unkat, S. (2020). A low-cost dual-axis solar tracking system based on digital logic design: Design and implementation. Sustainable Energy Technologies and Assessments, 37, 100618.
Kerekes, T., Teodorescu, R., Rodríguez, P., Vázquez, G., and Aldabas, E. (2009). A new high-efficiency single-phase transformerless PV inverter topology. IEEE Transactions on Industrial Electronics, 58(1), 184–191.
Komendantova, N., and Yazdanpanah, M. (2017). Impacts of human factors on willingness to use renewable energy sources in Iran and Morocco. Environmental Energy and Economic Research, 1(2), 141–152.
Letcher, T. M. (2018). Why Solar Energy? In A Comprehensive Guide to Solar Energy Systems. Elsevier.
Mousazadeh, H., Keyhani, A., Javadi, A., Mobli, H., Abrinia, K., and Sharifi, A. (2009). A review of principle and sun-tracking methods for maximizing solar systems output. Renewable and Sustainable Energy Reviews, 13(8), 1800–1818.
Nabi Bid Hendi, G., Daryabeigi Zand, A., and Rabiee Abyaneh, M. (2021). Assessing the Life-cycle Greenhouse gas (GHG) Emissions of Renewable and Fossil Fuel Energy Sources in Iran. Environmental Energy and Economic Research, 5(2), 1–9.

Outlook, B. P. E. (2020). energy outlook 2050. BP Publishers: London.
Ozcelik, S., Prakash, H., and Challoo, R. (2011). Two-axis solar tracker analysis and control for maximum power generation. Procedia Computer Science, 6, 457–462.
Rezaei, M. (2021). A Multi-Criteria Decision-Making Approach for Sustainable Energy Prioritization. Environmental Energy and Economic Research.
Rogelj, J., Den Elzen, M., Höhne, N., Fransen, T., Fekete, H., Winkler, H., et al. (2016). Paris Agreement climate proposals need a boost to keep warming well below 2 C. Nature, 534(7609), 631–639.
Sadeghi, S., and Vahidi, H. (2020). Using Floating Photovoltaics, Electrolyser and Fuel Cell to Decrease the Peak Load and Reduce Water Surface Evaporation. Environmental Energy and Economic Research, 4(2), 83–96.
Salehi, M., Khajehpour, H., and Saboohi, Y. (2019). Extended Energy Return on Investment of multiproduct energy systems. Energy, 116700.
Serrano-Luján, L., Espinosa, N., Abad, J., and Urbina, A. (2017). The greenest decision on photovoltaic system allocation. Renewable Energy, 101, 1348–1356.
Stritih, U. (2016). Increasing the efficiency of PV panel with the use of PCM. Renewable Energy, 97, 671–679.
Twidell, J., and Weir, T. (2015). Renewable energy resources. Routledge.
Wu, C.-H., Wang, H.-C., and Chang, H.-Y. (2022). Dual-axis solar tracker with satellite compass and inclinometer for automatic positioning and tracking. Energy for Sustainable Development, 66, 308–318.
Yousefi, H., Abbaspour, A., and Seraj, H. (2019). Worldwide development of wind energy and co2 emission reduction. Environmental Energy and Economic Research, 3(1), 1–9.
Zhang, Z., Pei, K., Sun, M., Wu, H., Yu, X., Wu, H., et al. (2020). A Novel Solar Tracking Model Integrated with Bistable Composite Structures and Bimetallic Strips. Composite Structures, 112506.